PROCEEDINGS OF SCIENCE

Measurement of photon and photon+jet production cross sections at 7 TeV and constraints to PDFs

Josu Cantero, on behalf of the ATLAS Collaboration
Universidad Autónoma de Madrid (UAM)
E-mail: josu.cantero.garcia@cern.ch

The inclusive isolated-photon production and the dynamics of isolated-photon plus jet production in pp collisions at a centre-of-mass energy of 7 TeV has been studied with the ATLAS detector at the LHC using an integrated luminosity of 4.5 fb^{-1} and 37 pb^{-1}, respectively. Measurements of the inclusive isolated-photon cross sections are presented as a function of the photon transverse energy and the impact of the measurements to constraint the gluon PDF is evaluated. Measurements of the isolated-photon plus jet differential cross sections are presented as functions of the photon transverse energy, the jet transverse momentum, the jet rapidity, the difference in azimuthal angle between the photon and the jet, the photon-jet invariant mass and the scattering angle in the photon-jet centre-of-mass frame. Next-to-leading-order QCD calculations are compared to the measurements and provide a good description of the data in both analyses, except in the case of the azimuthal angle.

XXII. International Workshop on Deep-Inelastic Scattering and Related Subjects,
28 April - 2 May 2014
Warsaw, Poland

PoS(DIS2014)160

ATL-PHYS-PROC-2014-055
17 June 2014

1. Introduction

Prompt photon production and the production of prompt photons in association with a jet at hadron colliders, $pp \to \gamma + \text{jet} + \text{X}$, provides a testing ground for perturbative QCD (pQCD) in a cleaner environment than in jet production since the photon originates from the hard interaction and does not undergo hadronisation.

The measurement is sensitive to the gluon content of the proton through the $qg \to q\gamma$ process, which dominates the prompt photon and prompt photon + jet production cross section at the LHC, and can be used to constrain parton distribution functions.

The dynamics of the underlying processes $2 \to 2$ hard collinear scattering can be investigated using the variable θ^*, $\cos\theta^* \equiv \tanh(\Delta y/2)$, where Δy is the difference in rapidity of the two final-state particles, and is sensitive to the spin of the exchanged particle.

At leading order (LO) in pQCD, the process in $pp \to \gamma + \text{jet} + \text{X}$ proceeds via two production mechanims: direct photons (DP), which originate from the hard process, and fragmentation photons (F), which arise from the fragmentation of a coloured high transverse momentum, p_T, parton [1, 2]. The photon was required to be isolated by using a criterium based on the amount of transverse energy inside a cone of radius 0.4 centred around the photon. The jets were defined using the anti-k_t jet algorithm [3] with distance parameter $R = 0.6$. In the case of the prompt photon production, the measurements were performed in the phase-space region of $E_T^\gamma > 100$ GeV, $|\eta^\gamma| < 2.37$ (excluding the region of $1.37 < |\eta^\gamma| < 1.52$), whereas for the production of prompt photon in association with a jet the phase space region of the measurements was $E_T^\gamma > 45$ GeV, $P_T^{\text{jet}} > 40$ GeV, $|y^{\text{jet}}| < 2.37$ and $\Delta R_{\gamma j} > 1$. The measurements of $d\sigma/dM^{\gamma j}$ and $d\sigma/d|\cos^{\gamma j}|$ were performed additionally for $|\eta^\gamma + y^{\text{jet}}| < 2.37$, $|\cos\theta^{\gamma j}| < 0.83$ and $M^{\gamma j} > 161$ GeV;

2. Isolated prompt photon production

2.1 Data selection and MC simulations

The measurement presented here is based on data collected at a center-of-mass energy of $\sqrt{s} = 7$ TeV with the ATLAS detector [4] at the LHC in 2011. Events are triggered using a high-level photon trigger, with a nominal E_T^γ threshold of 80 GeV. The total integrated luminosity of the collected sample is 4.6 fb^{-1}. Events were required to have a reconstructed primary vertex with at least three associated tracks, consistent with the average beam-spot position. The photon-candidate selection is based on the reconstruction of isolated electromagnetic clusters in the calorimeter. Clusters without matching tracks were classified as unconverted photons, whereas clusters matched to tracks were classified as converted photon candidates. The photon candidate was required to be isolated by restricting the amount of transverse energy around its direction ($E_{T,\text{det}}^{\text{iso}}$). The measured value of $E_{T,\text{det}}^{\text{iso}}$ was corrected by subtracting the estimated contributions from the underlying event and additional inelastic pp interactions [5]. After all these corrections, $E_{T,\text{det}}^{\text{iso}}$ was required to be below 7 GeV.

The MC programs PYTHIA 6.4 [6] and HERWIG 6.5 [7] were used to generate the signal events. The event-generator parameters, including those of the underlying-event modelling, were set according to the MRST2007 [8] and AUET2 [9] tunes for PYTHIA and HERWIG, respectively.

2.2 Background subtraction, signal-yield estimation and cross-section measurement procedure

A non-negligible background contribution remains in the selected sample. This background comes predominantly from QCD processes in which a jet is misidentified as a photon. A background subtraction method was devised which does not rely on MC background samples and uses instead signal-depleted control regions. The background contamination in the selected sample was estimated using the same two-dimensional sideband technique as in the previous analyses [5] and then subtracted bin-by-bin from the observed yield. The data distributions, after background subtraction, were corrected to the particle level using a bin-by-bin correction procedure.

2.3 Systematic uncertainties

Several systematic sources that affect the measurements were considered [10]. In the following the most important systematic sources are listed.

- Uncertainty on the photon energy scale (2% at low E_T^γ and 6% at large E_T^γ)
- Uncertainty on the model dependence ($\sim$2% at low E_T^γ to 4% at $E_T^\gamma > 800$ GeV)
- Uncertainty on the background subtraction, which varies between 2% and 3%

2.4 Next-to-leading-order QCD calculations

The NLO QCD calculations were computed using the program JETPHOX [11]. The renormalisation (μ_R), factorisation (μ_F) and fragmentation (μ_f) scales were chosen to be $\mu_R = \mu_F = \mu_f = E_T^\gamma$. The calculations were performed using the CT10 [12] and MSTW2008NLO [13] parametrisations of the proton PDFs and the NLO photon BFG set II photon fragmentation function [14]. The combined effect from hadronisation and the underlying events was estimated by using PYTHIA and HERWIG with different tunes and was found to be about $\pm$1%. The following sources of uncertainty in the theoretical predictions were considered: higher orders (varies between 12% and 20%); proton PDF (5% (15%) at $E_T^\gamma \approx 100$ GeV (900 GeV)); value of $\alpha_s(M_Z)$ ($\pm$4.5%).

2.5 Results

The measured E_T^γ-differential cross sections together with the theoretical predictions are shown in Figure 1. The NLO calculations agree with the data up to the highest E_T^γ considered. The data are somewhat higher than the central NLO calculation for low E_T^γ but agree within the theoretical uncertainty of the NLO calculation. At low E_T^γ the observed difference between the NLO predictions based CT10 PDF and MSTW2008NLO PDF are larger than the PDF uncertainty estimated using CT10.

2.6 Sensitivity to the proton parton distribution functions

The sensitivity of the data to the PDF can be assessed by comparing the measured cross sections to fixed order predictions based on different PDF sets. The HERAFITTER package [15] has been used to computed χ^2 values corresponding to the predictions for each PDF sets. Experimental systematic uncertainties and PDF uncertainties are included in the χ^2 calculation [16].
Comparison of the measured cross sections with the JETPHOX NLO QCD predictions using five different PDF sets are shown in Figure 2.

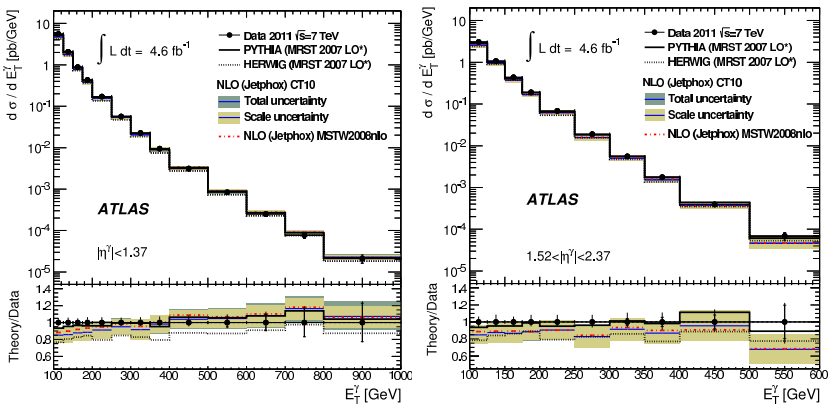

Figure 1: The measured differential cross section for isolated prompt photon (dots) as a function of E_T^γ for the barrel (left) and endcap (right) η^γ regions [10].

The results of the χ^2 tests indicate that there is a tension between the measured data and the predictions. Thus the data have great potencial to constraint both the shape and uncertainty of the gluon PDF. However, at intermediate E_T^γ where the data are most precise, the scale uncertainty is dominant. Therefore NNLO calculations may be necessary to fully exploit the measurement.

3. Isolated prompt photon + jet production

3.1 Data selection and MC simulations

The data were collected with the ATLAS detector during 2010, at a centre-of-mass energy of $\sqrt{s}$ = 7 TeV. Events were recorded using a single-photon trigger, with a nominal transverse energy threshold of 40 GeV. This trigger has an efficiency for photons with $E_T^\gamma > 45$ GeV and $|\eta^\gamma| < 2.37$ close to 100%. The total integrated luminosity of the collected sample amounts to 37.1 ± 1.3 pb^{-1}. Events were required to have a reconstructed primary vertex with at least five associated tracks. The $E_{T,\mathrm{det}}^{\mathrm{iso}}$ was required to be below 3 GeV. Jets were reconstructed from three-dimensional topological clusters built from calorimeter cells, using the anti-k_t algorithm with distance parameter $R = 0.6$. The jet four-momenta were computed from the sum of the jet constituent four-momenta, treating each as a four-vector with zero mass and then recalibrated using a jet energy-scale (JES) correction. Jets overlapping with the candidate photon or with an isolated electron were not considered. The requirement on the electrons suppresses contamination from W/Z plus jet events.
The MC programs PYTHIA 6.423 and HERWIG 6.510 were used to generate the signal events. The event-generator parameters, including those of the underlying-event modelling, were set according to the AMBT1 [17] and AUET1 [18] tunes for PYTHIA and HERWIG, respectively.
The measured differential cross sections refer to particle-level jets and photons which are isolated by requiring $E_{T,\mathrm{part}}^{\mathrm{iso}} < 4$ GeV in a cone of radius $R = 0.4$.

3.2 Background subtraction, signal-yield estimation and cross-section measurement procedure

A non-negligible background contribution remains in the selected sample. This background was subtracted by using the same data-driven technique explained in section 2.2. The data after

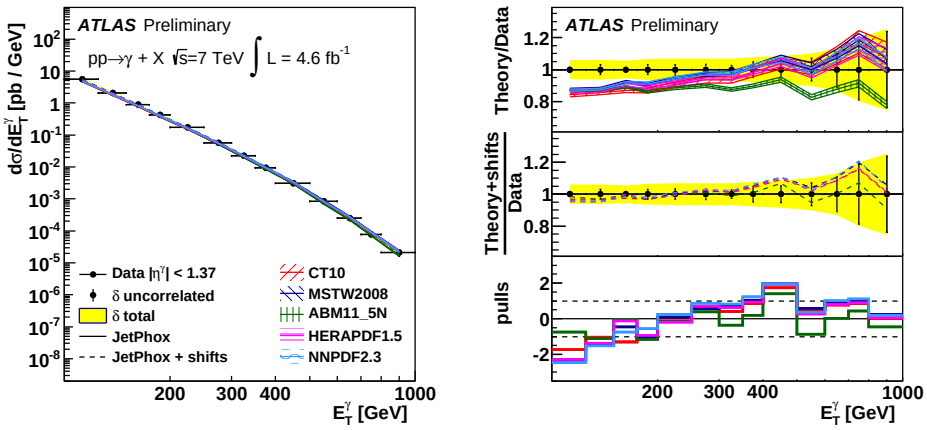

Figure 2: Measured cross section as a function of E_T^γ in the central $|\eta^\gamma| < 1.37$ pseudorapidity region compared to JETPHOX prediction with different PDF sets [16].

background subtraction were corrected to the particle level using a bin-by-bin correction procedure.

3.3 Systematic uncertainties

Several systematic sources that affect the measurements were considered [19]. In the following the most important systematic sources are listed. Average values, expressed in percent and shown in parentheses, quantify their effects on the cross section as a function of $|\cos\theta^{\gamma j}|$:

- simulation of the detector geometry ($\pm$5%).
- jet and photon energy scale. (photon energy scale: $\pm$1%; jet energy scale: $\pm$5%);
- uncertainty arising from the experimental isolation requirement (+4%).

3.4 Next-to-leading-order QCD calculations

The NLO QCD calculations were computed using the program JETPHOX. The calculations were performed using the CTEQ6.6 [20] parametrisations of the proton PDFs and the NLO photon BFG set II photon fragmentation function. The strong coupling constant was calculated at two loops with $\alpha_s(M_Z) = 0.118$. The NLO QCD predictions were corrected to the particle level by applying a multiplicative factor calculated from MC models. The following sources of uncertainty in the theoretical predictions were considered: higher orders ($\pm$14%); proton PDF ($\pm$3.5%); value of $\alpha_s(M_Z)$ ($\pm$2.5%) and the modelling of the QCD cascade, hadronisation and underlying event ($\pm$0.5%).

3.5 Results

The predictions of the NLO QCD calculations are compared to the data in Fig. 3. The predictions give a good description of the E_T^γ and P_T^{jet} measured cross sections. The NLO QCD calculation fails to describe the measured $\Delta\phi^{\gamma j}$ distribution, as expected due to the fact that in the NLO QCD calculation, the photon and the leading jet cannot be in the same hemisphere in the transverse plane, i.e. $\Delta\phi^{\gamma j} \geq \pi/2$. The leading-logarithm parton-shower prediction of PYTHIA gives a good description of the data in the whole range measured whereas HERWIG fails to describe the data.

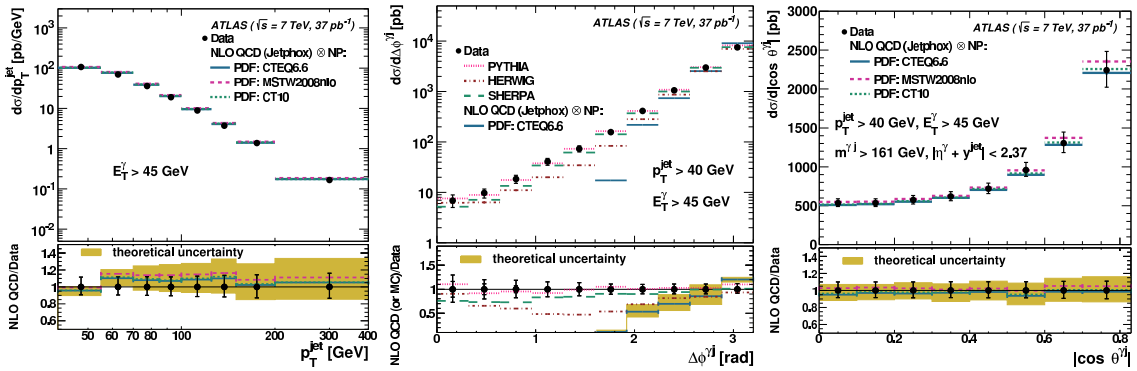

Figure 3: The measured differential cross section for isolated-photon plus jet production (dots) as a function of p_T^{jet} (left), $\Delta\phi^{\gamma j}$ (middle) and $|\cos\theta^{\gamma j}|$ (right) [19].

The measured cross sections as functions of $m^{\gamma j}$ and $|\cos\theta^{\gamma j}|$ are described well by the NLO QCD calculations.

References

[1] T. Pietrycki and A. Szczurek, Phys. Rev. **D 76,** 034003 (2007).

[2] Z. Belghobsi et al., Phys. Rev. **D 79,** 114024 (2009).

[3] M. Cacciari, G.P. Salam and G. Soyez, JHEP **0804,** 063 (2008).

[4] ATLAS Collaboration, JINST **3** (2008) S08003.

[5] ATLAS Collaboration, Phys. Rev. **D 83,** 052005 (2011).

[6] T. Sjöstrand, S. Mrenna and P.Z. Skands, JHEP **0605,** 026 (2006).

[7] G. Corcella et al., JHEP **0101,** 010 (2001).

[8] A.D. Martin, R. Roberts, W.J. Stirling and R. Thorne, Eur. Phys. J. C **4** 463 (1998).

[9] ATLAS Collaboration, ATL-PHYS-PUB-2011-008.

[10] ATLAS Collaboration, Phys. Rev. **D 89**, 052004 (2014)

[11] S. Catani et al., JHEP **0205,** 028 (2002).

[12] P.M. Nadolsky et al., Phys. Rev. **D 82,** 074024 (2010).

[13] A. Martin, W. Stirling, R. Thorne and G. Watt, Eur. Phys. J. **C 63**, 189 (2009).

[14] L. Bourhis, M. Fontannaz and J. Ph. Guillet, Eur. Phys. J. **C 2,** 529 (1998).

[15] H1 and ZEUS Collaboration, F. Aaron et al., JHEP **1001** 109 (2010).

[16] ATLAS Collaboration, ATL-PHYS-PUB-2013-018.

[17] ATLAS Collaboration, ATLAS-CONF-2010-031.

[18] ATLAS Collaboration, ATL-PHYS-PUB-2010-014.

[19] ATLAS Collaboration, Nucl. Phys, **B 875** (2013) 483-535.

[20] P. Nadolsky et al., Phys. Rev. **D 78,** 013004 (2008).